JOURNAL OF PROPULSION AND POWER
Vol. 22, No. 2, March–April 2006

Pulse Detonation Engine as a Ramjet Replacement

P. G. Harris* and R. A. Stowe*
Defence Research and Development Canada–Valcartier, Val-Bélair, Québec G3J 1X5, Canada
R. C. Ripley†
Martec, Ltd., Halifax, Nova Scotia B3J 3J8, Canada
and
S. M. Guzik‡
Defence Research and Development Canada–Valcartier, Val-Bélair, Québec G3J 1X5, Canada

System-level performance analyses of pulse detonation engines (PDE) have not demonstrated the same increases in performance, when compared to constant-pressure-based engine cycles, as those predicted by thermodynamic cycle analyses. This question is revisited in the present work, in which the performance of a PDE, based on specific impulse, is compared to that of a ramjet Mach 1.2 to 3.5. Using a constant-volume analytical model, event timing, geometric and injection parameters providing optimal performance were determined. These were then used as input to a one-dimensional model, based on the method of characteristics, and a two-dimensional model, based on computational fluid dynamics. The effect of partial fill and nozzle expansion ratio on specific impulse was also evaluated. For all models and over the range of Mach numbers considered, the specific impulse of the PDE was consistently greater than that of a ramjet. In addition, partial fill and nozzle expansion ratio were also identified as important factors influencing performance.

I. Introduction

THE mid-1980s mark the beginning of the most recent interest in the pulse detonation engine (PDE)[1,2] as a propulsion technology for missile systems. The PDE is a transient, detonation-based technology that operates on the principle of cyclical filling and detonation of a fuel/oxidizer mixture in a combustion chamber. Interest in the PDE has been primarily driven by its theoretical potential to provide significantly increased combustion efficiency (30 to 50%) over devices based on a constant-pressure process.[3] A major challenge in PDE research has been to determine how to transform this potential in combustion efficiency into increased propulsive efficiency while maintaining useful levels of thrust.

An idealized thermodynamic system analysis by Heiser and Pratt[4] based on a single value of the ratio of specific heats γ showed increases in the fuel-based specific impulse I_{sp} of the PDE cycle over that of the Brayton cycle. For values of the static temperature-rise ratio ψ less than 2, increases in the I_{sp} of the PDE cycle over the Brayton cycle of greater than 19% were obtained. For $2 < \psi < 3$, this increase was greater than 9%. Wu et al.[5] extended Heiser and Pratt's analysis to include two values of γ, one for the reactants and the other for the products. For $\psi < 2$, increases in the I_{sp} of the PDE cycle over the Brayton cycle of greater than 28% were obtained. For $2 < \psi < 3$ this increase was greater than 12%. The propulsive advantage of idealized PDEs has also been supported by the work of Dyer and Kaemming.[6] However, in general, experimental and numerical studies of specific PDE devices have not demonstrated these idealized performance advantages.

A significant body of experimental and theoretical work exists for single- and multicycle PDE devices with straight tubes and straight or diverging nozzles.[7–14] The I_{sp} generated with these devices, when the reactive mixture completely fills the detonation tube prior to initiation, is lower than what can be obtained by constant-pressure devices and considerably lower than the maximum performance predicted by thermodynamic analyses. In attempt to increase the I_{sp} of such devices, a portion of the detonation tube is filled with a nonreactive mixture. However, the resultant increase in I_{sp} is obtained at the cost of lowering thrust below useful levels.

In contrast to the thermodynamic system analysis of Heiser and Pratt, two different research groups carried out system-level performance analyses in which both component dimensions and timescales were considered. These studies confirmed the generally lower performance predictions of PDEs as compared to idealized thermodynamic analyses. At Pennsylvania State University (Penn State), a two-dimensional computational-fluid-dynamics (CFD) analysis was carried out for single- and multitube PDEs using a hydrogen-air mixture at a flight Mach number of 2.1 and altitude of 9.3 km (Refs. 5, 15, and 16). The maximum increase in I_{sp} reported over that of a ramjet for CFD simulations was 7% as compared to 27% based on a thermodynamic system analysis (Ma et al.[16]). This was for a PDE with a single tube and a converging-diverging nozzle. It was claimed that the nozzle throat increased performance by maintaining chamber pressure, but that the effect of the nozzle expansion ratio was minor. This latter conclusion is in contrast to the experimental work by Cooper and Shepherd,[17] where it was demonstrated that I_{sp} could be significantly enhanced by the diverging portion of a converging-diverging nozzle. At California Institute of Technology (Caltech), Wintenberger and Shepherd[18] used a two-dimensional CFD analysis combined with an analytical model to determine the performance of a nozzleless single-tube PDE. The effect of unsteady flow was modeled, such that the total pressure at the valve plane was lower than that downstream of the inlet. The I_{sp} of a nozzleless PDE was determined to be greater than that of a ramjet only up to a Mach number of 1.35.

A potential explanation for the discrepancy between the thermodynamic and system-level analyses is contained in the work of Talley and Coy.[19] They demonstrated that for a rocket engine based on constant-volume (CV) combustion performance efficiency gains with respect to a constant-pressure process were optimized when the minimum pressure in the combustion chamber was equal to the fill pressure. In both studies by Ma et al.[16] and Wintenberger and Shepherd,[18] the pressure in the combustion chamber during the complete fill cycle was significantly lower than the fill pressure. This was to be expected in the configuration used by Wintenberger and

Presented as Paper 2004-3744 at the AIAA/ASME/SAE/ASEE 40th Joint Propulsion Conference and Exhibit, Ft. Lauderdale, FL, 11–14 July 2004; received 5 January 2005; revision received 31 August 2005; accepted for publication 31 August 2005.

*Defence Scientist, Propulsion Group. Senior Member AIAA.
†Research Engineer, Combustion Dynamics Group. Member AIAA.
‡Military Attaché, Propulsion Group. Member AIAA.

Shepherd[18] because there was no converging nozzle on the detonation tube to maintain pressure. However, in the work reported by Ma et al.,[16] a converging-diverging nozzle was used, implying that any increase in I_{sp} could only be attained through system optimization.

The purpose of this paper is to revisit the system-level performance potential of a PDE by controlling average chamber pressure and nozzle expansion ratio. It will be demonstrated that for an idealized system the I_{sp} of a PDE is greater than that of ramjet over a large range of Mach numbers. Because no comparison with experimental data is presented as none are yet available in the open literature for this type of system, this work is proposed as a source of guidance for the design of future experiments. To provide a point of reference for the reader, the flight conditions and fuel/oxidizer system used in the work at Penn State were used in the present work. As such, the fuel/oxidizer system considered was H_2/air. The engine flight altitude was 9.3 km, and the baseline Mach number was 2.1; however, this was extended in the present study to include a range of Mach numbers.

II. System Concept and Modeling

The airbreathing system concept analyzed in this work (Fig. 1) assumes a quasi-steady inlet that feeds air into a plenum and then through multiple tubes. To facilitate performance optimization, tubes are isolated from each other at the upstream end by a valve and at the downstream end by a choked throat. In a flight version, the choked throat from individual tubes would vent into a common nozzle. However, in the present implementation each throat is connected to a separate diverging section.

The valves to the detonation tubes are opened either sequentially or in a regular overlapped fashion in order to ensure steady time-averaged flow through the system. Once the time-averaged mass flow rate is divided among the individual detonation tubes, the remainder of the analysis is carried out on a single-tube basis with the total impulse of the system being the product of the impulse of a single tube and the number of tubes. Pressure oscillations in the plenum are considered negligible from the performance perspective given the multitube nature of the system. Adiabatic, isentropic flow is generally assumed throughout the system except for total pressure losses associated with flow through the inlet and at the point of fuel injection. In addition, ideal valves that open and close instantaneously are assumed. Separate, but constant values of γ and R (particular gas constant) are used for each component mixture such that three sets of values corresponding to purge air, reactants, and products were used for most of the calculations reported.

A. Event Timing and Mass Flow Rate

Cycle time is defined as the sum of the time required for filling (valve open) and the time required for combustion and venting (valve closed):

$$\tau_{\text{cycle}} = \tau_{\text{open}} + \tau_{\text{closed}} \tag{1}$$

The time during which a valve is open is the sum of the time during which purge air is added and the time during which fuel is added to the air stream (refill):

$$\tau_{\text{open}} = \tau_{\text{purge}} + \tau_{\text{refill}} \tag{2}$$

Purge fraction is given as

$$\beta = \tau_{\text{purge}}/\tau_{\text{open}} \tag{3}$$

Initiation of combustion is assumed to occur immediately upon closing the valve. Definitions for time and purge fraction are the same as those in Ma et al.[16]

The time during which a tube valve is closed is related to the time it is open by

$$\tau_{\text{closed}} = (\varphi_S n_t - 1)\tau_{\text{open}} \tag{4}$$

where φ_s is the filling phase shift and n_t is the number of detonation tubes. To ensure that each valve is closed for a finite period of time and not immediately reopened after closing, the value of φ_s is constrained as

$$1 \geq \varphi_S \succ 1/n_t \tag{5}$$

These relationships are determined through deductive reasoning based on the assumption of identical event timing and time-averaged mass flow rates for each tube. The event timing is illustrated in Fig. 2 for $\varphi_s = 1.0$ and 0.5 and equal cycle times τ_{cycle}. For $\varphi_s = 1.0$, tubes are filled sequentially with only one valve opened at a time. For $\varphi_s = 0.5$, the time at which a valve is opened is offset by half the filling time.

The relationship between the time-averaged mass flow rate of air through each detonation tube and the entire engine is then given as

$$\bar{\dot{m}}_{\text{in}_{\text{system}}} = \bar{\dot{m}}_{\text{in}_{\text{tube}}}/\varphi_s \tag{6}$$

Fuel is injected at the valve plane based on the fuel-to-air ratio f. The time-averaged mass flow rate of reactants into a detonation tube during fuel injection is given as

$$\bar{\dot{m}}_{\text{reactants}} = (1 + f)\bar{\dot{m}}_{\text{in}_{\text{tube}}} \tag{7}$$

B. Boundary Conditions at the Valve Plane

As already mentioned, once the time-averaged mass flow rate is divided among the individual detonation tubes, the remainder of the analysis is carried out on a single-tube basis. This requires that the total pressure p_t and total temperature T_t at the valve plane be specified during the purge and fuel-injection portion of the fill cycle. Total conditions during the purge portion (station 2 in Fig. 1) are derived from flight conditions and are given as

$$p_{t2} = \eta_i p_{t0}, \qquad T_{t2} = T_{t0} \tag{8}$$

where η_i is the pressure recovery fraction that includes losses across the engine inlet and plenum.

Starting with Eq. (8), the total pressure p_{t3} and total temperature T_{t3} at the valve plane during fuel injection are specified based on the additional assumption that the fuel is injected perpendicularly to the flow; that is, no momentum is introduced by fuel injection. The total pressure loss associated with fuel injection is dependent on the Mach number of the air at the valve plane.

C. Performance Optimization

In accordance with Talley and Coy,[19] maximum I_{sp} is assumed to correspond to the operating condition where the pressure in each

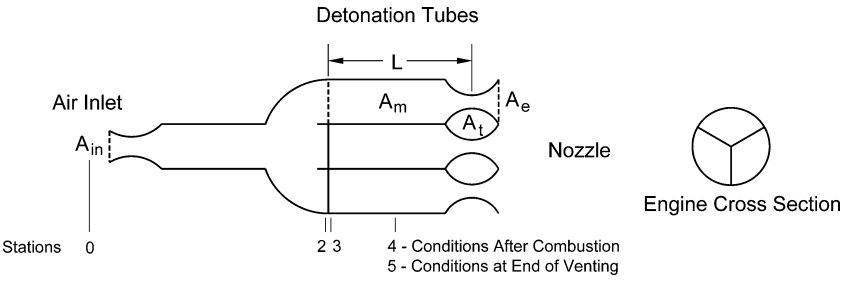

Fig. 1 Schematic of the PDE system concept.

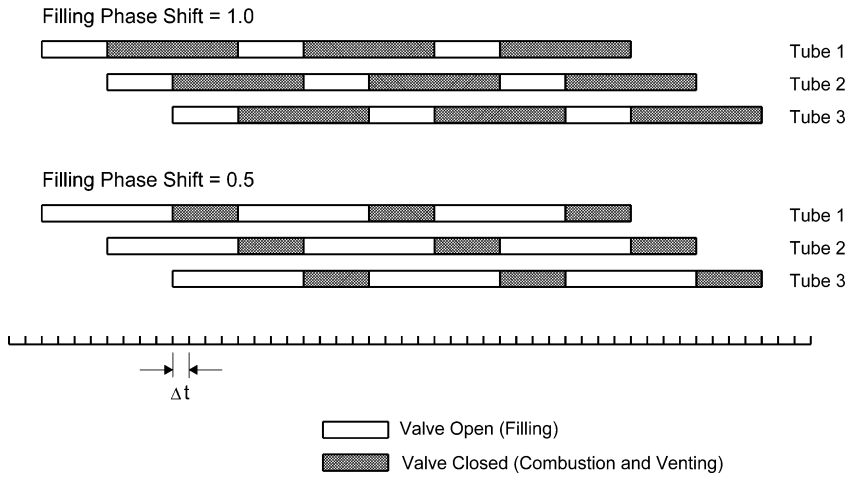

Fig. 2 Event timing scheme for two different values of φ_s.

detonation tube never drops below the fill pressure. Also, the exhaust gases are optimally expanded through a converging-diverging nozzle over the complete cycle.

Performance optimization, from the perspective of operating pressure, is performed in two steps. First, for a given time-averaged mass flow rate of air through the system, number of detonation tubes, and filling phase shift, the nozzle throat diameter D_t is iteratively adjusted such that at the end of a tube fill all mass from a previous cycle is completely vented and the pressure in the tube is equal to the fill pressure. Second, the pressure in each tube, at the instant the tube valve is opened, is iteratively adjusted to be equal to the fill pressure by varying φ_s. For PDEs with nozzle exit diameters D_e fixed throughout the cycle, once optimum values of D_t and φ_s have been calculated, D_e is iteratively varied to obtain maximum I_{sp} over a complete cycle.

D. Calculation of Thrust and Impulse

The behavior of each detonation tube is identical to that of the others except for an offset in time, so that the time-averaged axial thrust and impulse are calculated on the basis of a single tube. The system time-averaged value is simply the product of that for an individual tube and the number of tubes.

Given the different combustion model formulations (as described in the following chapter) and as a means of validating calculations, thrust was determined using two different methods. The first (method 1) is based on separate control volumes during the portion of the cycle that the valve of a tube is open and closed, and the second (method 2) is based on a single control volume for the entire cycle. A complete formulation of instantaneous thrust requires evaluation of the rate of change of momentum in the control volume with time. However, for cyclical operation

$$\int^{\tau_{\text{cycle}}} \frac{\partial}{\partial t} \int_{\Omega} \rho u \, \mathrm{d}V \, \mathrm{d}t = 0 \tag{9}$$

where ρ is the density, u is the axial velocity, and V is the volume. For integration, the control volume Ω refers only to the air inlet and the plenum for method 1. For method 2 it also includes the detonation tube and nozzle.

Based on Eq. (9), the rate of change of momentum was not included in the thrust equations in this chapter, and as such they are incomplete expressions of instantaneous thrust. Their usefulness, however, is gleaned from the definition of impulse over an entire cycle.

The control volumes for method 1 are illustrated in Fig. 3 for tube 1. During the time that the valve is closed, thrust for the detonation tube is based on a single control volume around the detonation tube. During the time that the valve is open, a second control volume is needed, which includes the portion of the plenum and inlet that supplies air to tube 1. The portion of the inlet included in the control

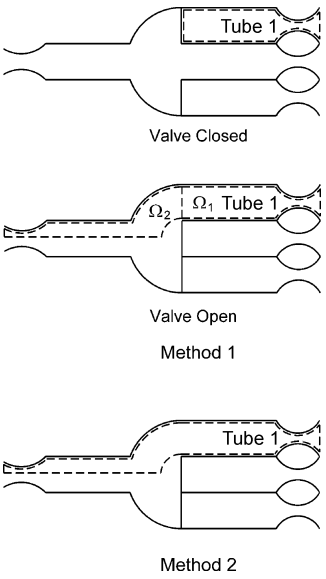

Fig. 3 Schematic of control volumes used in the thrust calculation methods 1 and 2. The actual proportion of the inlet area included in the control volume for an individual tube depends on φ_s.

volume is determined by φ_s and includes the entire inlet for $\varphi_s = 1$. The axial thrust during the time that the valve is closed and open can be given as

$$F_{\text{closed}} = \int_{\text{valve}} p \, \mathrm{d}A - \int_{\text{converging}} p \, \mathrm{d}A + \int_{\text{diverging}} p \, \mathrm{d}A - p_0 A_{\text{exit}} \tag{10}$$

$$F_{\text{open}} = \int_{\text{valve}} p \, \mathrm{d}A - \int_{\text{converging}} p \, \mathrm{d}A + \int_{\text{diverging}} p \, \mathrm{d}A - p_0 A_{\text{exit}} + \int_{\text{valve}} \rho u u \, \mathrm{d}A - \bar{\dot{m}}_{\text{in}_{\text{tube}}} u_0 \tag{11}$$

where p is the pressure, A is the cross-sectional area perpendicular to the tube axis, p_0 is the static pressure of ambient air, and u_0 is the engine flight velocity.

The time-averaged mass flow rate of air into a detonation tube is given as

$$\bar{\dot{m}}_{\text{in}_{\text{tube}}} = \int^{\tau_{\text{open}}} \dot{m}_{\text{in}_{\text{tube}}} \, \mathrm{d}t \Big/ \tau_{\text{open}} \tag{12}$$

The control volume for the complete cycle based on method 2 is also shown in Fig. 3. The axial thrust for method 2 can be given as

$$F = \int_{\text{exit}} \rho u u \, \mathrm{d}A - \bar{\dot{m}}_{\text{in}_{\text{tube}}} u_0 + (p_{\text{exit}} - p_0) A_{\text{exit}} \tag{13}$$

where the time-averaged mass flow rate of air is given as

$$\bar{\dot{m}}_{\text{in}_{\text{tube}}} = \int^{\tau_{\text{open}}} \dot{m}_{\text{in}_{\text{tube}}}\,\mathrm{d}t \Big/ \tau_{\text{cycle}} \tag{14}$$

The impulse over a cycle is given as

$$I = \int^{\tau_{\text{cycle}}} F\,\mathrm{d}t \tag{15}$$

and the fuel-based specific impulse is given as

$$I_{\text{sp}} = I/gm_f \tag{16}$$

where g is the acceleration caused by gravity and m_f is the mass of fuel injected.

Finally, the average axial thrust for a tube and the entire system is given as

$$\bar{F}_{\text{tube}} = I/\tau_{\text{cycle}}, \qquad \bar{F}_{\text{system}} = n_t \bar{F}_{\text{tube}} \tag{17}$$

and the specific thrust for the system is given as

$$F_{\text{sp}} = \bar{F}_{\text{system}}/\bar{\dot{m}}_{\text{in}_{\text{system}}} \tag{18}$$

III. Detonation Tube Modeling

The combustion and gas dynamics processes of an individual detonation tube were modeled, and the results integrated into the system analysis framework, detailed in the preceding section, for the calculation of system performance. The modeling of the individual detonation tubes was performed in three different ways. First, an analytical model based on CV combustion was developed to calculate event timing and tube and nozzle geometry required for optimal performance. These values were in turn used as input to the other models. Second, a one-dimensional model based on the method of characteristics (MOC) and a Chapman–Jouget (CJ) detonation wave solution using the thermochemical equilibrium code Chemkin II[20] accounted for detonative combustion and transient gas dynamics effects, which were not included in the CV analytical model. This provided a more complete description of the physics than the CV analytical model at reasonable computational costs. Finally, two-dimensional flow effects were modeled with a CFD description of the flowfield along with a single-step constant-reaction time (CRT) model for CJ detonation waves.

The use of the analytical model for performance optimization represented a compromise in methodology. On one hand, computation times for optimization were significantly reduced as compared to optimization based on the MOC or CFD models. On the other hand, the absence of transient gas dynamic effects and detonative combustion in the analytical model results in combinations of event timing and physical dimensions that are not completely optimal when used with the more complex models.

Simple detonation models were chosen for the MOC and CFD simulations for three reasons. First, the emphasis of the present work was on idealized performance characterization, as opposed to a detailed study of detonation phenomenon that would have included such issues as initiation, deflagration-to-detonation transition (DDT), and detonation cell size. As such, the level of complexity of the detonation models in the present work is similar to that of Wu et al.[5] Second, experimental work[8] has shown that the impulse-generating capacity of a DDT is similar to that of a direct initiation, as assumed in the present work. Third, the computational load involved in full multispecies multireaction finite-rate chemistry simulations is very costly for multicycle calculations.

A. Analytical Model

The formulation of the analytical model is an extension of the rocket engine work by Talley and Coy[19] to account for airbreathing systems and multiple values of γ and R. The present formulation also includes a model for partial fill, where varying amounts of purge air separate the reactants from the hot combustion products.

The heat added during the CV combustion process is given as

$$q = [R_4/(\gamma_4 - 1)]T_4 - [R_3/(\gamma_3 - 1)]T_3 \tag{19}$$

where state 3 corresponds to the conditions of the fuel/air mixture prior to combustion, and state 4 corresponds to the conditions of the combustion products immediately after combustion. Values of γ, R, and T_4 are calculated with the NASA Lewis Research Center thermochemical equilibrium code (CEA),[21] and as such q is not the lower heating value as reported by other authors.[4]

For cases with partial fill, the compression of the purge gas (prior to venting) by the high-pressure combustion products is modeled by two constant-volume processes. First, the combustion products perform isentropic work on the purge gas until a condition of equal pressure is attained. However, in order for this to occur, work is extracted from the closed system as the interface between the two mixtures is displaced. Therefore, a second process is required where the extracted work energy is reinserted. This is modeled by a heat addition process to the purge gas, where the pressure of the purge gas and combustion products remain equal throughout the process. This combination of processes is not as efficient as a transient compression process, and, as such, the performance of the analytical model deteriorates relative to the other models as the time-based purge fraction increases. This could be remedied by the addition of empirical constants to the compression model.

B. MOC Model

The MOC model was chosen over a one-dimensional finite difference implementation because of the advantage of being able to start the detonation calculation without imposing an initiation region at high pressure and high temperature. The practical result is that the impulse calculations with the MOC model do not vary with chamber length. As with the analytical model, each component mixture is assigned its own values of γ and R. Detonation is modeled as a CJ detonation wave and is calculated with the thermochemical equilibrium code Chemkin II.[20]

Event timing, tube and nozzle geometry, and total conditions at the valve plane are all input from the analytical model. For a more complete explanation of the MOC model, the reader is referred to Guzik et al.[22]

C. CFD Model

The CFD simulation was performed using the Chinook code, developed by Martec, Ltd. Chinook is a parallelized explicit unstructured-mesh finite volume code that solves a coupled system of hyperbolic conservation laws for mass, momentum, energy, and component mixture concentration. The governing equations are the Euler equations with source terms:

$$\frac{\partial \boldsymbol{U}}{\partial t} + \nabla \cdot \boldsymbol{F} = \boldsymbol{S} \tag{20}$$

where $\boldsymbol{U}$, $\boldsymbol{F}$, and $\boldsymbol{S}$ are vectors of conservative variables, inviscid fluxes, and source terms respectively, defined as follows for two-dimensional flow:

$$\boldsymbol{U} = \begin{bmatrix} \rho \\ \rho u \\ \rho v \\ \rho e \\ \rho \boldsymbol{Y}_i \end{bmatrix}, \qquad \boldsymbol{F} = V_n \begin{bmatrix} \rho \\ \rho u \\ \rho v \\ \rho e + p \\ \rho \boldsymbol{Y}_i \end{bmatrix} + p \begin{bmatrix} 0 \\ n_x \\ n_y \\ 0 \\ 0 \end{bmatrix}$$

$$\boldsymbol{S} = \frac{\lambda v}{r} \begin{bmatrix} \rho \\ \rho u \\ \rho v \\ \rho e \\ \rho \boldsymbol{Y}_i \end{bmatrix} + \begin{bmatrix} 0 \\ 0 \\ 0 \\ S_e \\ S_i \end{bmatrix} \tag{21}$$

In Eq. (21), ρ is the density, u and v are the Cartesian velocity components, e is the total specific energy, $\boldsymbol{Y}$ is a vector of mass fractions

for each component mixture continuity equation, p is the pressure, V_n is the face-normal velocity, and n_x and n_y are normal vector components. The source-term vector contains both geometric and reaction source terms. The variable λ is used to select the geometric coordinate system where $\lambda = 0$ for planar and $\lambda = 1$ for axisymmetric flow about the x axis. The sources S_e and S_i are involved with the detonation model and represent the source of energy through combustion and mass transfer between component mixtures respectively.

Based on calculations with CEA, each component mixture is assigned its own values of γ and R that are held constant throughout the calculation. The ideal-gas law, with the mixed ratio of specific heats γ_{mix}, is used to close the coupled system of equations:

$$p = \rho(\gamma_{\text{mix}} - 1)\left[e - \tfrac{1}{2}(u^2 + v^2)\right] \tag{22}$$

Mixture rules are employed for the gas constant $R = \Re / W_{\text{mix}}$, where $\Re = 8314\ \text{J/(kmol K)}$ is the universal gas constant. The molecular mass W_{mix} and ratio of specific heats γ_{mix} of a multicomponent gas mixture containing m components are determined using

$$W_{\text{mix}} = 1 \Big/ \sum_i^m \frac{Y_i}{W_i}, \quad \gamma_{\text{mix}} = 1 \Big/ W_{\text{mix}} \sum_i^m \frac{Y_i}{W_i(\gamma_i - 1)} + 1 \tag{23}$$

Detonation is modeled using a one-step CRT burn model,[23,24] which assumes that the reactants and products can be represented as independent gas component mixtures. This simple reaction model converts the global reactant mixture into a product gas component mixture, while adding energy to the system, to produce a supersonic combustion wave traveling at the detonation velocity. In the one-step CRT model, the heat of combustion q is defined implicitly as

$$M_{\text{CJ}} = \sqrt{\frac{\gamma_4^2 - 1}{2}\frac{q}{c_3^2} - \frac{\gamma_4 + 1}{2\gamma_3}\frac{\gamma_3 - \gamma_4}{\gamma_3 - 1}} + \sqrt{\frac{\gamma_4^2 - 1}{2}\frac{q}{c_3^2} - \frac{\gamma_4 + 1}{2\gamma_3}\frac{\gamma_3 - \gamma_4}{\gamma_3 - 1} + \frac{\gamma_4}{\gamma_3}} \tag{24}$$

where properties at states 3 and 4, as well as M_{CJ}, are calculated with CEA. Heat is released at a fixed rate given that a specified ignition temperature T_{ig} has been attained. The source terms corresponding to the CRT reaction model are

$$S_p = -S_f = \begin{cases} \rho R_{\text{fcr}} & \text{for} \quad T > T_{\text{ig}} \\ 0 & \text{otherwise} \end{cases}$$

$$S_e = q S_p \tag{25}$$

where the subscripts p, f, and e denote source terms for the products component mixture, fuel component mixture, and energy conservation equations, respectively. The mass fuel consumption rate R_{fcr} is given as

$$R_{\text{fcr}} = D_{\text{CJ}}/l \tag{26}$$

where D_{CJ} is the detonation wave speed and l is the physical length over which the energy is released, that is, the length of the reaction zone. Initial values of l are chosen based on experimental data. The model is then tuned by varying the l until the correct CJ and Taylor wave parameters are obtained in the CFD solution.

The equations of motion are applicable to inviscid compressible flow for non-heat-conducting gases and are solved using the Godunov method. The Harten, Lax, Van Leer, contact wave (HLLC)[25] high-speed convection scheme is used in the flux solver and provides high resolution of shocks and discontinuities at the material interfaces. The HLLC flux solver provides an approximate solution to the Riemann problem at each cell interface in the mesh using a two-state, three-wave approach. Properties employed in the flux solver, such as the speed of sound, are determined based on the gas mixture properties. The Chinook code employs two-dimensional unstructured, hybrid meshes allowing for mesh-aligned boundaries with a high level of control for local mesh resolution. Fluxes are calculated at each face in the mesh, and a discretized form of Eq. (20) is advanced in time using a time step chosen for solution stability. Second-order spatial accuracy is provided using second-order corrections with Green–Gauss gradients, which are limited by a MinMod limiter to prevent oscillations in the solution.

Event timing, tube and nozzle geometry, and total conditions at the valve plane are all input from the analytical model.

IV. Analytical Ramjet Model

An analytical model of an ideal ramjet was developed as a comparison with PDE performance calculations. It was based on the principles found in standard propulsion texts,[26] with the addition of multiple values of γ and R. As such, a detailed development is not presented in this paper. As with the PDE system, the only losses taken into account are those associated with total pressure recovery through the inlet and the plenum and the injection of fuel perpendicular to an airstream. The heat added during the constant-pressure combustion process is given as

$$q = [\gamma_4 R_4/(\gamma_4 - 1)]T_4 - [\gamma_3 R_3/(\gamma_3 - 1)]T_3 \tag{27}$$

where the temperatures and values of γ and R are calculated with CEA.

V. Model Validation

To establish confidence in the system performance predictions, both analytical and CFD models were validated. The MOC model was already validated extensively.[22]

A. Analytical Model Validation

The results from the CV (also referred to as the Humphrey cycle throughout this chapter) and ramjet analytical models were compared with those obtained from Wu et al.'s[5] thermodynamic analysis. The values of γ_1, γ_2, and $q/C_{p1}T_0$ from Wu et al.[5] were 1.4, 1.18, and 22.47, respectively, where C_{p1} is the specific heat at constant pressure for the reactants. Calculations with our CV and ramjet models were adjusted to give a low-Mach-number flow through the engine thereby minimizing injection losses and the effect of static-pressure decrease on performance. In addition, as in Wu et al.,[5] complete expansion through the nozzle was assumed. For the CV model this required that the nozzle exit diameter be varied throughout the cycle. Finally, parallel flow at the nozzle exit plane was assumed (nozzle cone divergence half-angle α of zero). The variation of I_{sp} with Mach number is compared in Fig. 4 for the different models. The results from Wu et al.'s[5] formulation of the PDE cycle are also included for reference. Agreement between the two sets of models is very good,

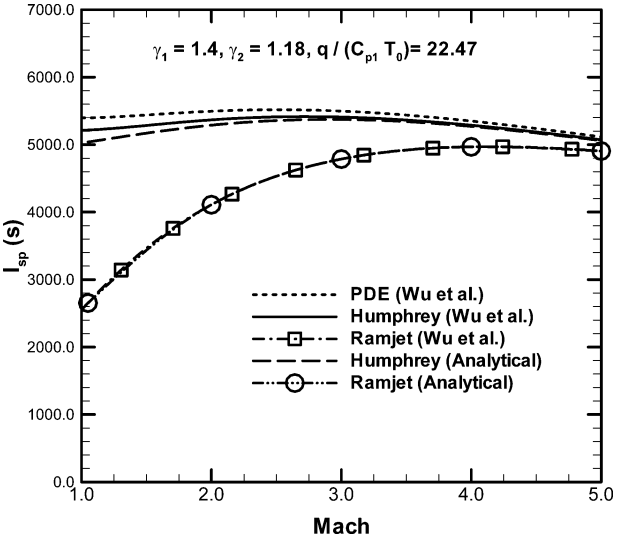

Fig. 4 Comparison of I_{sp} obtained with the present analytical models and those from Wu et al.[5] (The Brayton cycle in Wu et al. has been identified here as a ramjet cycle.)

with the results for the ramjet cycle being almost identical over the range of the Mach numbers and the maximum difference for the Humphrey cycle being less than 3.5%.

B. CFD Model Validation

A one-dimensional grid-sensitivity study was performed to evaluate the CRT detonation model. The detonation wave speed, CJ pressure, and temperature were calculated with CEA. The pressure and temperature behind the Taylor wave were calculated analytically. All parameters were compared with the results from the Chinook simulations. Grid sizes of 0.6, 0.3, 0.15, 0.075, and 0.0375 mm were studied. For a grid of 0.6 mm, all Chinook parameters were within 0.55% of the CEA and analytical values. The difference decreased to 0.3% for a grid of 0.15 mm and to below 0.2% for grids 0.075 mm and smaller, so that the solution was considered as completely converged on a 0.075-mm grid.

The CRT detonation model was also compared with finite-rate chemistry calculations. The propagation of a one-dimensional detonation wave in a stoichiometric mixture of H_2/O_2 with nitrogen dilution was evaluated using the commercial code CFD++[27] with a 27-step, 12-species reaction mechanism from Yungster and Radhakrishnan[28] based on the classic Jachimowski scheme.[29] The grid size for the calculation was 0.035 mm. The initiation region for both the Chinook and finite-rate calculations was identical. The pressure-time profiles for Chinook and the finite-rate calculations are compared in Fig. 5 at four locations. Agreement is very good justifying use of the simple approach.

Two-dimensional axisymmetric grid-sensitivity studies were performed for a single detonation in a straight tube and for multicycle operation of a tube with a converging-diverging nozzle. The purpose was to evaluate whether the solution convergence trend identified in the one-dimensional study held for the calculation of I_{sp} in two-dimensional configurations. The straight tube was 60 cm long and 6 cm in diameter. The geometry of the tube with the converging-diverging nozzle was the baseline condition for the system performance analysis to be presented in the next chapter (Mach = 2.1). Initial pressure and temperature conditions for both tubes were also those of the baseline condition. Grid sizes of 0.6, 0.3, and 0.15 mm were studied. The solution convergence trends based on I_{sp} were the same as those for the one-dimensional grid-sensitivity study. Because of the significant increase in computation time with grid refinement for multicycle PDE calculations, it was decided to carry out system performance analyses with a grid size of 0.6 mm. For this grid size the system performance parameters are estimated to be approximately 0.55% above the converged solution.

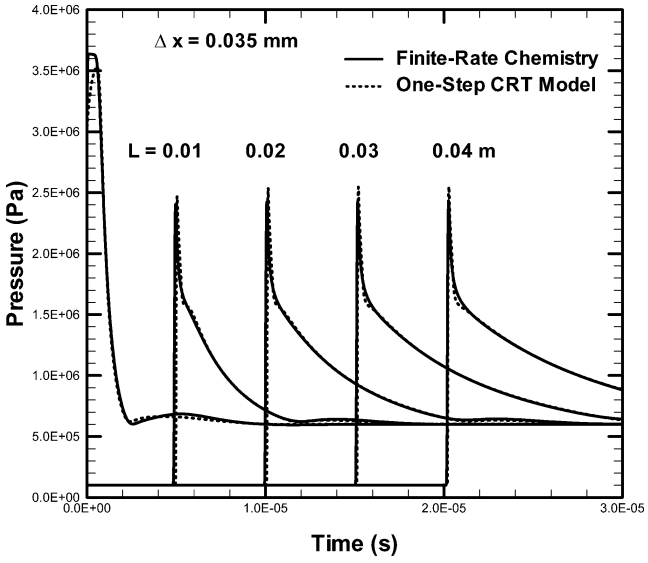

Fig. 5 Comparison of pressure-time profiles for the one-step CRT detonation model in Chinook and finite-rate chemistry calculations with CFD++.

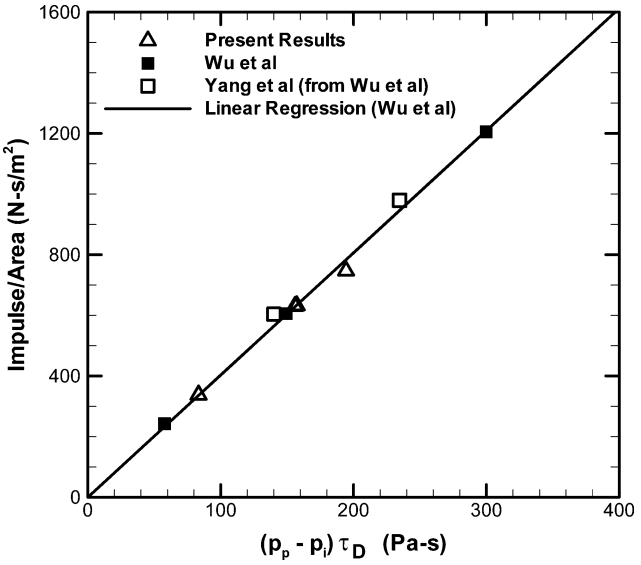

Fig. 6 Comparison of the impulse per unit area from a single detonation in a straight tube between the present results and those from Wu et al.[5]

Chinook calculations were also validated by comparison with external sources. The results from single-cycle calculations with the straight tube geometry from the preceding paragraph are compared in Fig. 6 with results from Wu et al.[5] A linear relationship is established between impulse per unit area and $(p_p - p_i)\tau_D$, where p_p is the pressure at the closed end of the tube after the Taylor expansion wave, p_i is the initial pressure, and τ_D is the time required for the detonation wave to travel the tube length. This linear relationship is significant in the present context of validation, in that it is similar to an expression proposed by Wintenberger et al.[11] based on experimental data, and has also been confirmed by Kailasanath[13] in numerical simulations. The initial temperature and pressure in the detonation tube for two of the three cases were the same as those of the reactants for flight conditions of Mach 1.2 and 2.1 in the system performance analysis. Initial conditions for the third case were 101 325 Pa and 298 K. Stoichiometric H_2/air mixtures were used in all of the calculations. The mixture was initiated by a region of combustion products, 0.6 mm long, at twice the CJ pressure and 2000 K. As with the calculations of Wu et al.,[5] impulse was calculated up until the time that the pressure at the closed end of the detonation tube fell below the initial pressure. Based on testing, the contribution of the detonation initiation region to the impulse is estimated to be less than 0.2%. Agreement between the Chinook calculations and those by Wu et al.[5] is good.

To validate Chinook calculations for multicycle operation, and to validate the data-reduction procedure by which the CFD results were transformed into system performance values, the baseline geometry for a single tube PDE from Ma et al.[16] was modeled. Flight conditions were Mach 2.1 at 9.3 km. Total pressure and total temperature in the freestream were 268 500 Pa and 428 K, respectively. A total pressure drop across the inlet and the plenum of 20% was assumed such that the total pressure at the valve plane during filling was 214,800 Pa. Single values of γ and R of 1.29 and 368.9 J/(kg K) were used as opposed to multiple values as in the system performance simulations in the next chapter, the effect of which will also be discussed. The variation of I_{sp} and F_{sp} as a function of the time the valve is closed is compared in Fig. 7 for calculations with Chinook and by Ma et al.[16] Both axisymmetric and planar calculations are presented. Agreement in the results is very good, providing confidence in the multicycle Chinook calculations and the data-reduction procedure.

VI. System Performance Analysis

The system performance of a multicycle three-tube PDE is evaluated in this section and compared to that of a ramjet.

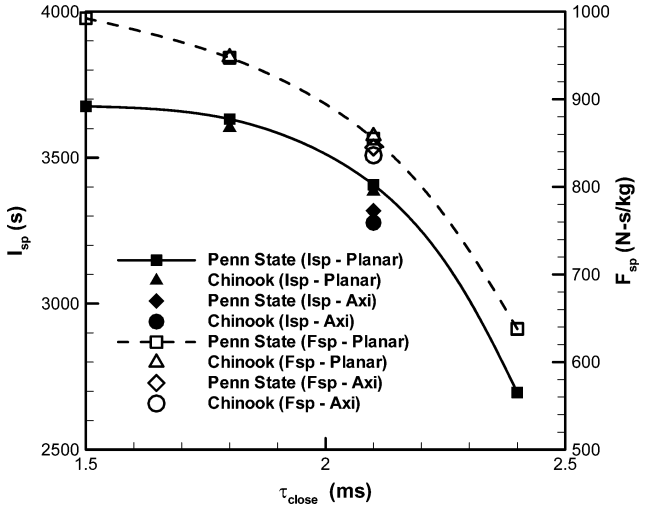

Fig. 7 Comparison of I_{sp} and F_{sp} for a single-tube multicycle PDE as calculated with Chinook and by Ma et al.[16]

A. Calculation Matrix

To facilitate comparison, the baseline flight conditions, pressure recovery fraction, and fuel/oxidizer system were chosen to match those used in the work at Penn State. As such, the baseline flight conditions were Mach 2.1 at 9.3 km, the pressure recovery fraction was 0.8, and the fuel/oxidizer system was stoichiometric H_2/air. Analytical, MOC, and CFD calculations were also performed at Mach 1.2, 3.0, and 3.5. To illustrate extended performance trends, analytical and MOC calculations were also performed for Mach 4.0 and 5.0. However, CFD calculations were not performed in this flight regime because the total temperature in the detonation chamber exceeded that of the autoignition temperature of the mixture (858 K) making practical implementation of a PDE very difficult. For the present altitude, this temperature is exceeded at Mach 3.7. No temperature limitation in the detonation tube was applied to any of the calculations.

The effect of partial fill on I_{sp} was evaluated by performing calculations for two values of time-based purge fraction, $\beta = 0.04$ and 0.25. In addition, the effect of nozzle expansion ratio was also evaluated for the baseline test case, Mach 2.1 and $\beta = 0.4$.

The time-averaged mass flow rate through the system for each test case was chosen to generate useful time-averaged thrust levels. As such, the time-averaged thrust chosen for the baseline flight Mach number was equivalent to that produced by the single-tube PDE in Ma et al.[16] For the other flight Mach numbers, thrust levels were originally scaled from the baseline by accounting for a change in drag at the new flight Mach number. However, cycle times based on these thrust levels would have resulted in excessively long numerical calculation times. As such, the cycle periods were adjusted to be approximately equal to that of the baseline test case. The thrust levels generated for this condition were significantly higher than those based on extrapolation of the baseline thrust level, resulting in conservative conditions for the performance evaluation. The Mach 1.2 flight condition represented an exception to this general rule in that the level of thrust based on drag adjustment was not attained (neither for the PDE nor the ramjet) given high combustor Mach numbers. The time-averaged thrust levels for $\beta = 0.04$ and 0.25 are shown in Figs. 8 and 9, respectively.

The geometric parameters for the different test cases, as calculated with the CV analytical model, are given in Table 1. The definitions of the diameters, lengths, and angles specified in the table are illustrated in Fig. 10. The motor diameter D_m and the nozzle cone divergence half-angle α were 8.44 cm and 15 deg respectively for all test cases. Event timings, and values of φ_s, are given in Table 2, thermodynamic parameters as a function of Mach number and combustion model are contained in Table 3, and valve interface and detonation initiation total pressure and total temperature are presented in Table 4. For all CFD calculations, the initiation region

Table 1 Geometric engine tube and nozzle parameters for different test cases

Test case	Mach number	β	D_t, cm	D_e, cm	L_{tb}, cm[a]	L_e, cm[a]	θ, deg[a]
1	1.2	0.04	3.75	4.36	65.22	1.40	45.0
2	2.1	0.04	4.82	4.82	64.71	0.000	45.0
3	2.1	0.04	4.82	5.90	64.71	2.28	45.0
4 (baseline)	2.1	0.04	4.82	7.84	64.71	5.90	45.0
5	3.0	0.04	4.46	11.38	64.88	13.17	45.0
6	3.5	0.04	4.37	13.83	64.92	17.90	45.0
7	4.0	0.04	4.07	16.28	NA[b]	NA[b]	NA[b]
8	5.0	0.04	3.98	25.17	NA[b]	NA[b]	NA[b]
9	1.2	0.25	4.09	4.66	65.05	1.33	45.0
10	2.1	0.25	5.42	8.39	63.55	5.81	45.0
11	3.0	0.25	4.94	11.79	64.66	13.05	45.0
12	3.5	0.25	4.73	14.33	64.75	18.17	45.0
13	4.0	0.25	4.47	16.71	NA[b]	NA[b]	NA[b]
14	5.0	0.25	4.37	23.31	NA[b]	NA[b]	NA[b]

[a]Applies only to two-dimensional CFD calculations, where L_{tb} was calculated such that the chamber volume up to the nozzle throat was equal to that of the CV analytical and MOC calculations. For the CV analytical and MOC calculations the length of the tube was 63.473 cm.
[b]No CFD simulations were performed for these Mach numbers.

Table 2 Event timing and filling phase shift for different test cases

Mach number	β	φ_s	τ_{cycle}, ms	τ_{purge}, ms	$\tau_{reactants}$, ms	τ_{closed}, ms	Cycle frequency, Hz
1.2	0.04	1.000	16.493	0.220	5.280	10.993	60.6
2.1	0.04	0.879	8.639	0.131	3.149	5.359	115.8
2.1	0.04	0.879	8.639	0.131	3.149	5.359	115.8
2.1	0.04	0.879	8.639	0.131	3.149	5.359	115.8
3.0	0.04	0.833	8.401	0.142	3.219	5.040	119.0
3.5	0.04	0.795	7.941	0.143	3.189	4.609	126.0
4.0	0.04	0.758	8.393	0.158	3.535	4.700	119.2
5.0	0.04	0.678	7.272	0.155	3.420	3.697	137.5
1.2	0.25	0.960	13.793	1.197	3.593	9.003	72.5
2.1	0.25	0.824	6.745	0.682	2.048	4.015	148.3
3.0	0.25	0.765	6.952	0.757	2.273	3.922	143.8
3.5	0.25	0.720	6.907	0.799	2.401	3.707	144.8
4.0	0.25	0.705	7.169	0.847	2.543	3.779	139.5
5.0	0.25	0.630	6.274	0.830	2.490	2.954	159.4

extended across the whole tube diameter and was 0.6 mm thick. The static pressure and temperature for ambient air was 2.94×10^4 Pa and 227.7 K respectively for all calculations. For the sake of brevity, the ramjet thermodynamic and geometric parameters have not been included.

B. CFD Computational Domain and Grid

The standard CFD computational domain used in the calculations is illustrated in Fig. 11. The straight portion of the detonation tube (region 1) contained a structured quadrilateral mesh with dimensions $\Delta x = \Delta y = 0.6$ mm. The converging and diverging portions of the nozzle (region 2) contained a triangular unstructured mesh with 0.8-mm edges. The region starting at the nozzle exit (region 3) contained a triangular unstructured mesh, starting with 0.8-mm edges and growing to 12.5-mm edges in the far field. High mesh refinement was maintained in region 3 only near the nozzle exit plane, as the rest of the computational domain was included to ensure correct boundary conditions at the nozzle exit plane.

C. Sample Results

The behavior of the PDE in the time domain is illustrated in this chapter using sample results from the baseline test case, Mach 2.1 and $\beta = 0.04$.

Pressure at the valve interface for the CV analytical, MOC, and CFD (Chinook) calculations is shown in Fig. 12. The MOC and CFD results are very similar showing transient shock behavior, whereas the CV analytical pressure resembles a time average of the transient results. The pressure at the valve interface is permitted to fall below

Table 3 Thermodynamic parameters for the different test cases

Mach number	Comb. model	Air		Reactants		Products		
		γ	R, J/(kg K)	γ	R, J/(kg K)	γ	R, J/(kg K)	q, J/Kg
1.2	CV	1.400	287.04	1.402	395.78	1.164	344.49	5.436×10^6
2.1	CV	1.400	287.04	1.394	395.78	1.169	344.20	5.328×10^6
3.0	CV	1.400	287.04	1.378	395.78	1.173	344.31	5.242×10^6
3.5	CV	1.400	287.04	1.365	395.78	1.174	344.61	5.199×10^6
4.0	CV	1.400	287.04	1.351	395.78	1.175	345.12	5.163×10^6
5.0	CV	1.400	287.04	1.326	395.78	1.176	346.80	5.068×10^6
1.2	CJ	1.400	287.04	1.402	395.78	1.159	347.20	5.628×10^6
2.1	CJ	1.400	287.04	1.395	395.78	1.164	346.86	5.508×10^6
3.0	CJ	1.400	287.04	1.379	395.78	1.169	346.80	5.379×10^6
3.5	CJ	1.400	287.04	1.366	395.78	1.171	347.07	5.309×10^6
4.0	CJ	1.400	287.04	1.352	395.78	1.173	347.57	5.243×10^6
5.0	CJ	1.400	287.04	1.327	395.78	1.176	349.31	5.084×10^6

Table 4 Conditions at the valve interface and initiation region (for detonative combustion)

Mach number	Purge		Reactants		Initiation region	
	P_t, Pa	T_t, K	P_t, Pa	T_t, K	P_t, Pa	T_t, K
1.2	5.70×10^4	293.3	5.60×10^4	295.1	1.67×10^6	2000
2.1	2.15×10^5	428.5	2.08×10^5	434.3	4.14×10^6	2000
3.0	8.64×10^5	637.9	8.47×10^5	641.5	1.22×10^7	2000
3.5	1.79×10^6	785.6	1.76×10^6	789.1	2.12×10^7	2000
4.0	3.57×10^6	956.4	3.53×10^6	958.8	NA[a]	NA[a]
5.0	1.24×10^6	1366.3	1.23×10^6	1368.2	NA[a]	NA[a]

[a]No CFD calculations were done for these conditions.

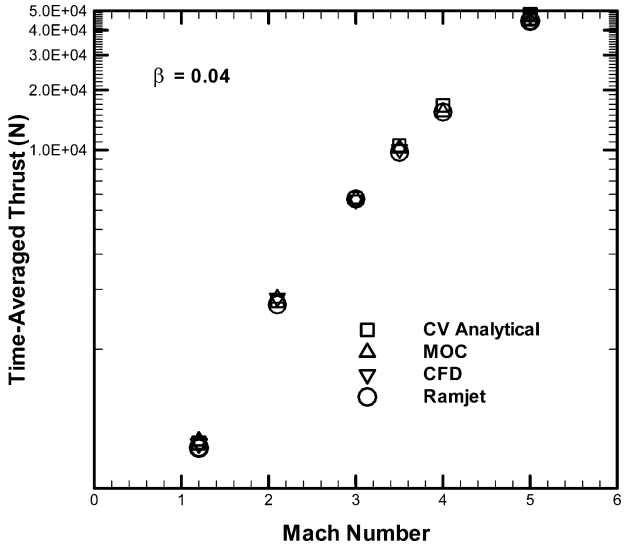

Fig. 8 Time-averaged thrust as a function of Mach number for $\beta = 0.04$.

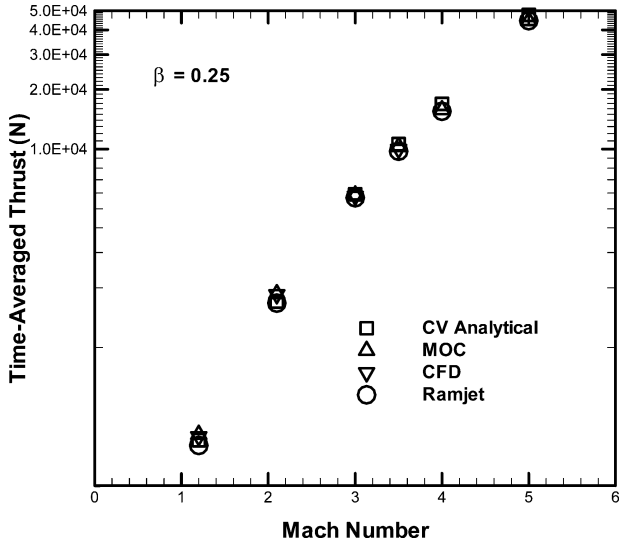

Fig. 9 Time-averaged thrust as a function of Mach number for $\beta = 0.25$.

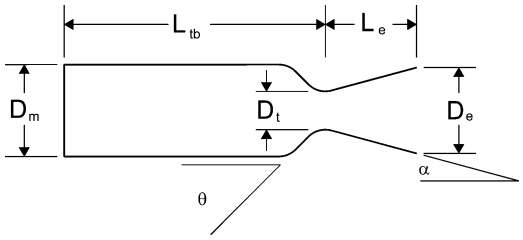

Fig. 10 Illustration of the definition of geometric variables for Table 1.

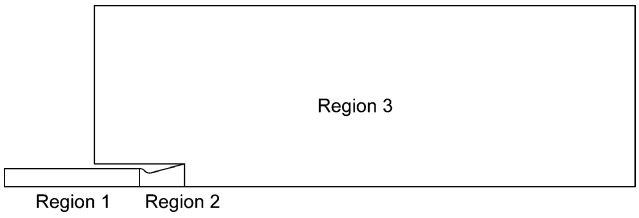

Fig. 11 Standard computational domain.

the specified total fill pressure p_{3t} corresponding to fuel injection. This was done by design for all test cases to ensure that reflected shock waves at the beginning of the fill process did not cause the MOC and CFD calculations to fail because of the outflow of combustion products at the valve interface. Therefore, the average pressure in the detonation tube was lower than the maximum possible value, with the consequence that values of I_{sp} reported in this paper for PDE performance are below maximum possible values.

Thrust profiles for the CFD calculations using methods 1 and 2 are shown in Fig. 13. A comparison of the thrust profiles for the CV analytical, MOC, and CFD calculations is not included because the level of agreement follows that for the pressure profile at the valve interface (Fig. 12). Although the instantaneous value of thrust for the two methods varies considerably in Fig. 13, the total impulse over one cycle differs by less than 0.3%. This illustrates the preceding assertion that the values of thrust as defined by Eqs. (10), (11), and (13) are not complete descriptions of the instantaneous thrust of the PDE system but are meaningful as time-averaged values over a cycle. The good agreement between the two methods also serves to build confidence in the thrust calculations.

Contour plots of the absolute value of the density gradient for two different times in a cycle are shown in Figs. 14 and 15. The times

correspond to those from the pressure plot in Fig. 12. Figure 14 shows the detonation wave just prior to its arrival at the nozzle entrance. The oblique shock wave at the nozzle exit indicates that the exhaust gases are highly expanded at the end of the fill cycle. However, there is no normal shock in the nozzle expansion cone. Upon striking the nozzle entrance cone, the detonation wave generates a strong reflected shock wave that travels upstream towards the valve plane. This is illustrated in Fig. 15 along with the spherical shock wave resulting from the failed detonation, propagating from the nozzle exit plane. The spherical shock wave is elongated along the axis of symmetry as a result of burning of spilted fuel. A detailed and complete description of the flow physics can be found in Ma et al.[16]

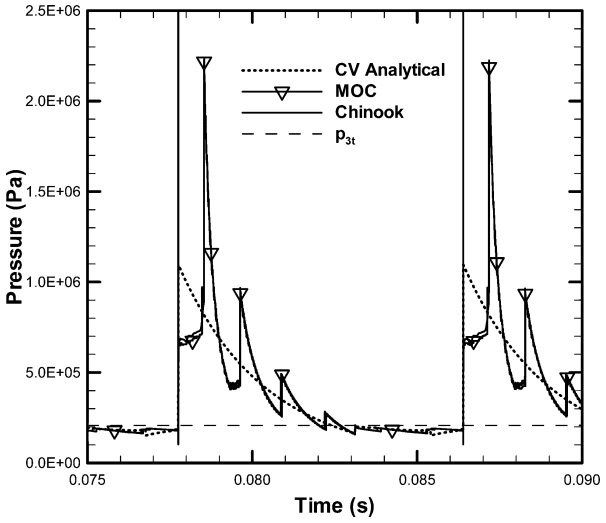

Fig. 12 Pressure at the valve interface for the baseline condition, Mach 2.1 and $\beta = 0.04$, for the three different modeling approaches.

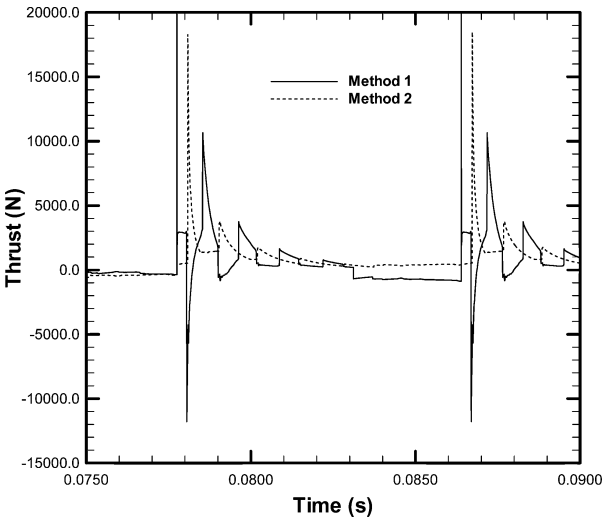

Fig. 13 Thrust as calculated by methods 1 and 2 for the baseline condition, Mach 2.1 and $\beta = 0.04$.

D. Variation of I_{sp} with Flight Mach Number

As a point of reference for the performance of the different test cases in Table 1, curves of maximum I_{sp} were calculated based on the CV analytical and ramjet models. These calculations were similar to those illustrated in Fig. 4 in that they assumed low flow Mach-number velocities, complete expansion of the nozzle exhaust gases, no purge, and parallel flow at the nozzle exit plane. However, as for the different test cases, γ, R, and q were varied with Mach number based on CEA. The resulting curves of maximum I_{sp} are compared in Fig. 16 with the model from Wu et al.[5] in Fig. 4. The figure indicates that although the overall trend remains the same use of varying parameters significantly affects the detailed behavior.

The values of I_{sp} for the different test cases and combustion models from each system analysis are compared with those for a ramjet in Figs. 17 and 18 for $\beta = 0.04$ and 0.25, respectively. Curves of maximum I_{sp} are also included for reference. In both Figs. 17 and 18, results from all three models follow similar trends and indicate that the I_{sp} of the PDE system is greater than that of the ramjet over the complete range of Mach numbers. For $\beta = 0.04$ and Mach numbers of 1.2, 2.1, 3.0, and 3.5, the I_{sp} of the PDE (based on CFD) exceeds that of the ramjet by 105, 22, 10, and 5%, respectively. For $\beta = 0.25$ this difference increases to 126, 31, 19, and 13%, which is consistent with the effect of purge identified by other authors. The highest value of I_{sp} for the PDE reported by Ma et al.[16] is also included in the figures for reference. At only 7% greater than that of a ramjet, the I_{sp} of Ma et al.[16] is significantly smaller than the value obtained in this study for the corresponding Mach number. As mentioned earlier, results at Mach 4.0 and 5.0 were omitted from the present discussion since the total temperature in the detonation tube during fill exceeds that of the autoignition temperature of H_2/air.

The agreement between the results for the CV analytical and CFD models for $\beta = 0.04$ in Fig. 17 is within 2%, with agreement within 5.5% for $\beta = 0.25$ in Fig. 18. As mentioned earlier, the increased difference for $\beta = 0.25$ results from the inefficiency (relative to an unsteady process) of the quasi-steady processes used in the CV analytical model to describe the compression of the purge gas by the high-pressure combustion products. Agreement with the MOC and CFD models could be increased by incorporating empirical constants in the CV analytical model.

The difference between the results for the MOC and CFD models for $\beta = 0.04$ in Fig. 17 is generally within 1.4%, although for Mach 1.2 the difference was 3.9%. For $\beta = 0.25$ in Fig. 18, the difference is generally within 2.4%, although for Mach 3.5 the difference was 3.7%. As would be expected, the agreement between the MOC and CFD models was superior to that between CV analytical and CFD models. In particular, the prediction of the effect of purge by the MOC model was superior to that of the CV analytical model.

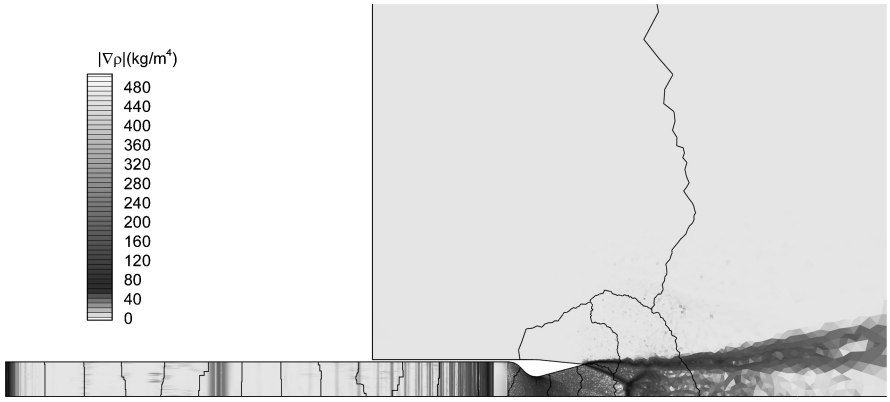

Fig. 14 Density gradient of the flowfield for the baseline condition immediately before the detonation wave reaches the converging portion of the nozzle ($t = 0.07803$ corresponds to Fig. 12).

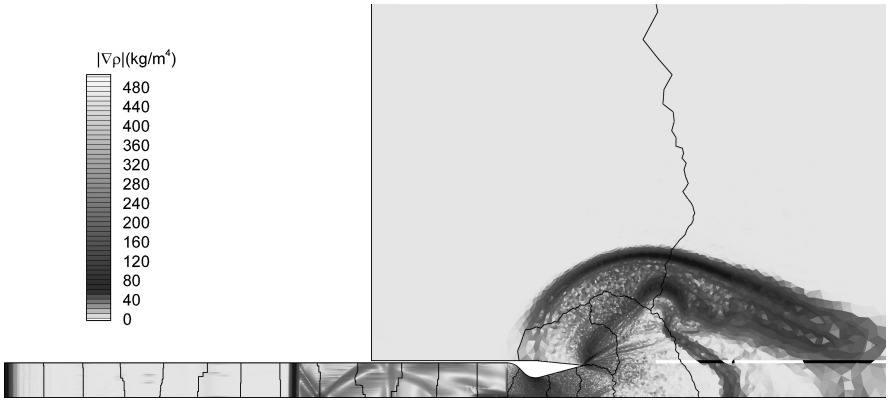

Fig. 15 Density gradient of the flowfield for the baseline condition after the detonation wave has exited the nozzle ($t = 0.07829$ corresponds to Fig. 12).

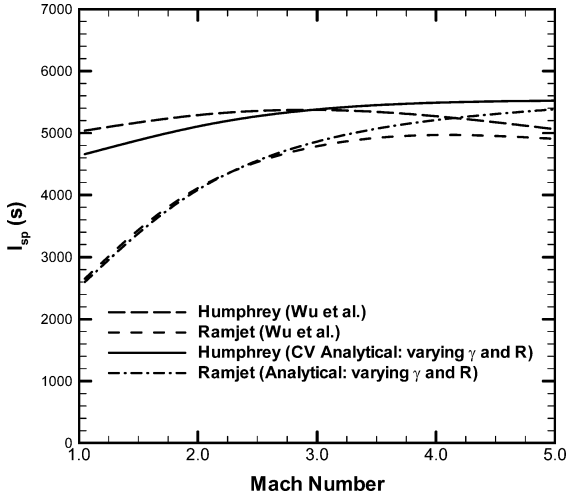

Fig. 16 Comparison of the Humphrey and ramjet models from Wu et al.[5] with the analytical models from the present work for γ, R, and q varied with Mach number.

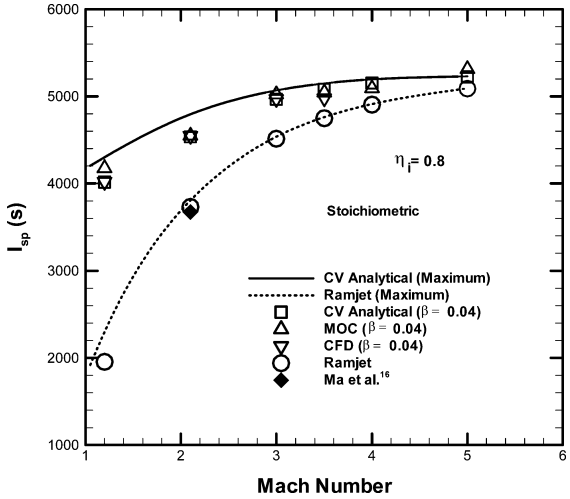

Fig. 17 I_{sp} of the PDE system and ramjet for $\beta = 0.04$ for the three different modeling approaches.

E. Variation of I_{sp} with Nozzle Expansion Ratio

The effect of nozzle expansion ratio ε on I_{sp} was evaluated with the CV analytical, MOC, and CFD models by varying the nozzle exit diameter of the baseline test case. The results in Fig. 19 show that the dependence of I_{sp} on ε is significant with I_{sp} increasing by 20% when ε was increased from 1.0 to 2.65. This behavior is similar to that of standard steady flow systems, like rocket engines. As such, as the flight Mach number and thus the average total pressure in a detonation tube increases, the effect of ε increases. Ma et al.[16] might have missed this effect because they chose values of ε that were in the flatter portion of the curve.

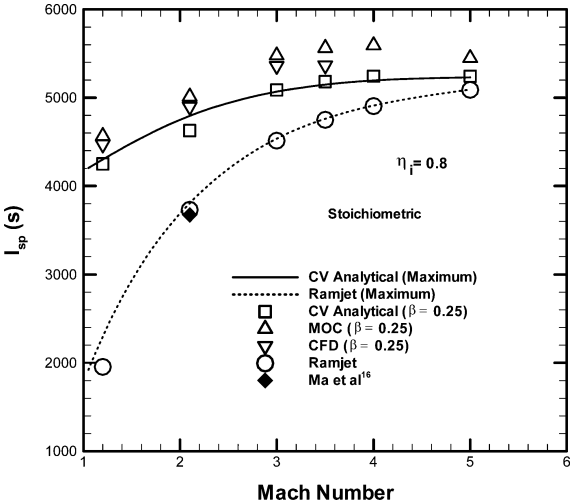

Fig. 18 I_{sp} of the PDE system and ramjet for $\beta = 0.25$ for the three different modeling approaches.

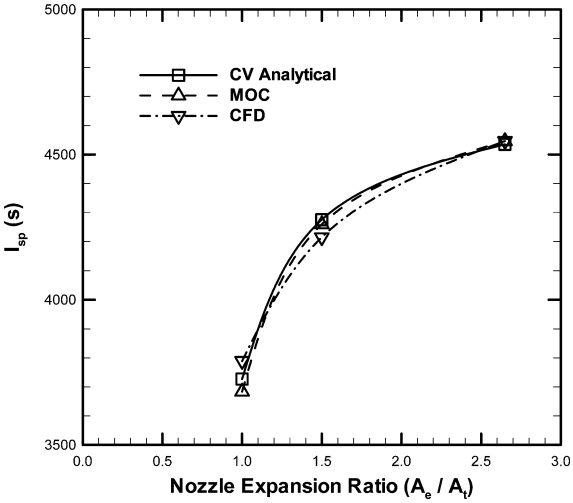

Fig. 19 Effect of nozzle expansion ratio on I_{sp} for the PDE for the baseline condition for the three different modeling approaches.

F. Comparison of Results with Penn State

The present analysis produced values of I_{sp} of 4547 and 4898 s at the baseline flight condition for $\beta = 0.04$ and 0.25, respectively. These values are 24 and 33% greater than the maximum reported

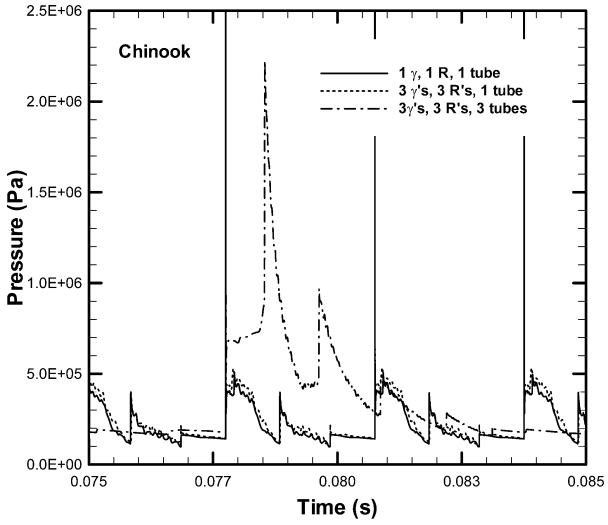

Fig. 20 Evolution of pressure profiles for the Penn State geometry as calculation parameters are modified.

by the group at Penn State, 3672 s (Ref. 16). This difference can be attributed to two major factors. First, the Penn State calculations assumed single values of γ and R, where in the present calculations three different sets of values were assumed to account for the different properties of air, reactants, and combustion products. The effect of this difference in choice of parameters on pressure at the valve interface is illustrated in Fig. 20 for one and three sets of parameters using the identical tube design and injection conditions as in Ma et al.[16] These calculations were performed with Chinook with $\tau_{\text{closed}} = 2.1$ ms. The average pressure over a cycle is 8.7% greater for the calculation with three sets of parameters as compared to one. This increase in pressure, accompanied by a variation in mass flow characteristics through the engine resulted in a 28% increase in I_{sp}, from 3277 to 4206 s. The large increase in I_{sp} compared to that of the average pressure resulted primarily from the important part that $p_0 A_e$ and the pressure integral in the nozzle expansion cone play in the calculation of thrust; $p_0 A_e$ did not change for the two calculations, and the pressure integral in the nozzle expansion cone increased by 19.5%. Second, in the present calculations, event timing and tube and nozzle geometry were modified based on the CV analytical model to ensure operation at near optimal average pressure. A typical pressure trace at the valve interface for this case, three values of γ and R and three detonation tubes, is also illustrated in Fig. 20. The average pressure for this case is 61% higher than for the case with three values of γ and R and a nonoptimized single tube geometry and timing scheme. The I_{sp} is between 8 and 16% greater, depending on the amount of purge.

VII. Conclusions

The system-level performance of an idealized PDE, as defined by I_{sp}, was compared with that of a ramjet over a range of flight Mach numbers. For the PDE, event timing, geometric, and injection parameters were chosen with a CV analytical model, which were in turn used in one-dimensional MOC and two-dimensional CFD (Chinook) simulations. The trends from all models were consistent and showed that for useful thrust levels the I_{sp} from a PDE is superior to that of a ramjet over a large range of Mach numbers. Consistent with work from other authors, a significant effect of purge (partial fill) was also demonstrated. Based on the results from the CFD simulations at Mach numbers of 1.2, 2.1, 3.0, and 3.5, the I_{sp} of the PDE was 105, 22, 10, and 5% greater than that of a ramjet for $\beta = 0.04$, and 126, 31, 19, and 13% greater for $\beta = 0.25$. Finally, the importance of nozzle expansion ratio in the process of performance optimization was also demonstrated.

The results presented in this work are consistent with trends for ideal performance as identified by Heiser and Pratt, as well as Dyer and Kaemming, and provide a resolution to the problem of low values of I_{sp} identified by the Penn State[5,15,16] and Caltech groups.[18]

No comparison with experimental data was presented in this paper as none is available in the open literature for this type of system. The methodology in this work is therefore proposed as a source of guidance for the design of future experiments.

Acknowledgments

The authors would like to sincerely thank Fuhua Ma and Vigor Yang of The Pennsylvania State University for the significant help they provided by supplying conditions and results for their computational-fluid-dynamics simulations. Thanks also go to Shaye Yungster for providing details for his chemical reaction model of hydrogen/air.

References

[1]Helman, D., Shreeve, R. P., and Eidelman, S., "Detonation Pulse Engine," AIAA Paper 1986-1683, July 1986.

[2]Eidelman, S., Grossmann, W., and Lottati, I., "Review of Propulsion Applications and Numerical Simulations of the Pulsed Detonation Engine Concept," *Journal of Propulsion and Power*, Vol. 7, No. 6, 1991, pp. 857–865.

[3]Bussing, T., and Pappas, G., "Pulse Detonation Engine Theory and Concepts," *Developments in High-Speed-Vehicle Propulsion Systems*, edited by S. N. B Murthy and E. T. Curran, Vol. 165, Progress in Astronautics and Aeronautics, AIAA, Reston, VA, 1996, pp. 421–472.

[4]Heiser, W. H., and Pratt, D. T., "Thermodynamic Cycle Analysis of Pulse Detonation Engines," *Journal of Propulsion and Power*, Vol. 18, No. 1, 2002, pp. 68–76.

[5]Wu, Y., Ma, F., and Yang, V., "System Performance and Thermodynamic Cycle Analysis of Airbreathing Pulse Detonation Engines," *Journal of Propulsion and Power*, Vol. 19, No. 4, 2003, pp. 556–567.

[6]Dyer, R. S., and Kaemming, T. A., "The Thermodynamic Basis of Pulsed Detonation Engine Thrust Production," AIAA Paper 2002-4072, July 2002.

[7]Zitoun, R., and Desbordes, D., "Propulsive Performance of Pulsed Detonations," *Combustion Science and Technology*, Vol. 144, Nos. 1–6, 1999, pp. 93–114.

[8]Harris, P. G., Farinaccio, R., Stowe, R. A., Higgins, A. J., Thibault, P. A., and Laviolette, J.-P., "The Effect of DDT Distance on Impulse in a Detonation Tube," AIAA Paper 2001-3467, July 2001.

[9]Cooper, M., Jackson, S., Austin, J., Wintenberger, E., and Shepherd, J. E., "Direct Experimental Impulse Measurements for Detonations and Deflagrations," *Journal of Propulsion and Power*, Vol. 18, No. 5, 2002, pp. 1033–1041.

[10]Kiyanda, C. B., Tanguay, V., Higgins, A. J., and Lee, J. H. S., "Effect of Transient Gasdynamic Processes on the Impulse of Pulse Detonation Engines," *Journal of Propulsion and Power*, Vol. 18, No. 5, 2002, pp. 1124–1126.

[11]Wintenberger, E., Austin, J. M., Cooper, M., Jackson, S., and Shepherd, J. E., "Analytical Model for the Impulse of Single-Cycle Pulse Detonation Tube," *Journal of Propulsion and Power*, Vol. 19, No. 1, 2003, pp. 22–38.

[12]Wintenberger, E., Austin, J. M., Cooper, M., Jackson, S., and Shepherd, J. E., "Analytical Model for the Impulse of Single-Cycle Pulse Detonation Tube," *Journal of Propulsion and Power*, Vol. 20, No. 4, 2004, pp. 765–767.

[13]Kailasanath, K., "Recent Developments in the Research on Pulse Detonation Engines," *AIAA Journal*, Vol. 41, No. 2, 2003, pp. 145–159.

[14]Li, C., and Kailasanath, K., "Partial Fuel Filling in Pulse Detonation Engines," *Journal of Propulsion and Power*, Vol. 19, No. 5, 2003, pp. 908–916.

[15]Ma, F., Wu, Y., Choi, J.-Y., and Yang, V., "Thrust Chamber Dynamics and Propulsive Performance of Multitube Pulse Detonation Engines," *Journal of Propulsion and Power*, Vol. 21, No. 4, 2005, pp. 681–691.

[16]Ma, F., Choi, J.-Y., and Yang, V., "Thrust Chamber Dynamics and Propulsive Performance of Single-Tube Pulse Detonation Engines," *Journal of Propulsion and Power*, Vol. 21, No. 3, 2005, pp. 512–526.

[17]Cooper, M., and Shepherd, J. E., "The Effect of Transient Nozzle Flow on Detonation Tube Impulse," AIAA Paper 2004-3914, July 2004.

[18]Wintenberger, E., and Shepherd, J. E., "A Model for the Performance of Air-Breathing Pulse Detonation Engines," AIAA Paper 2003-4511, July 2003; *Journal of Propulsion and Power* (to be published).

[19]Talley, D. G., and Coy, E. B., "Constant Volume Limit of Pulsed Propulsion for a Constant γ Ideal Gas," *Journal of Propulsion and Power*, Vol. 18, No. 2, 2002, pp. 400–406.

[20]Kee, R. J., Miller, J. A., and Jefferson, T. H., "CHEMKIN: General-Purpose, Problem-Independent, Transportable, Fortran Chemical Kinetics Code Package," Sandia National Lab., Rept. 80-8003, 1980.

[21]Gordon, S., and McBride, B. J., "Computer Program for Calculation of Complex Chemical Equilibirum Compositions and Applications," NASA RP 1311, Oct. 1994.

[22]Guzik, S. M., Harris, P. G., and De Champlain, A., "An Investigation of Pulse Detonation Engine Configurations Using the Method of Characteristics," AIAA Paper 2002-4066, July 2002.

[23]Korobeinikov, V. P., Levin, V., Markov, V. V., and Chernyi, G. G., "Propagation of Blast Waves in a Combustible Gas," *Astronautica Acta*, Vol. 17, 1972, pp. 529–537.

[24]Ripley, R. C., Josey, T., Donahue, L., and Whitehouse, D. R., "Shock Wave Interactions with Detonable Clouds," *Proceedings of the 12th Annual Conference of the CFD Society of Canada*, CFD2004, May 2004, pp. 109, 110.

[25]Batten, P., Clarke, N., Lambert, C., and Causon, D. M., "On the Choice of Wavespeeds for the HLLC Riemann Solver," *Siam Journal of Scientific Computing*, Vol. 18, No. 6, 1997, pp. 1553–1570.

[26]Hill, P., and Peterson, C., *Mechanics and Thermodynamics of Propulsion*, Addison Wesley Longman, Reading, MA, 1992, pp. 155–160.

[27]Goldberg, O., Peroomian, O., Chakravarthy, S., and Sekar, B., "Validation of CFD++ Code Capability for Supersonic Combuster Flowfields," AIAA Paper 97-3271, July 1997.

[28]Yungster, S., and Radhakrishnan, K., "Computational and Experimental Study of Nox Formation in Hydrogen-Fueled Pulse Detonation Engines," AIAA Paper 2004-3307, July 2004.

[29]Jachimowski, C. J., "An Analytical Study of the Hydrogen-Air Reaction Mechanism with Application to Scramjet Combustion," NASA TP-2791, Feb. 1988.